Proceedings of 14th IOE Graduate Conference
Peer Reviewed
Year: 2023 Month: December Volume: 14
ISSN: 2350-8914 (Online), 2350-8906 (Print)

Coupled Torsional And Transverse Vibration Analysis Of Double Overhung Rotor Shaft Centrifugal Fan

Sujan Dahal [a], Prajwal Raj Shakya [b], Madhav Kandel [c], Mahesh Chandra Luintel [d]

[a, b, c] *Department of Automobile and Mechanical Engineering, Thapathali Campus, IOE, Tribhuvan University, Nepal*
[d] *Department of Aerospace and Mechanical Engineering, Pulchowk Campus, IOE, Tribhuvan University, Nepal*
[a] sujand458@ioepc.edu.np, [b] pshakya@tcioe.edu.np, [c] madhav_5004@tcioe.edu.np, [d] mcluintel@ioe.edu.np

Abstract
The disk attached to a shaft is the basic component of various rotating mechanical equipment. When in use, these are bent and twisted. The coupled effect of lateral and torsional vibration is a frequent cause of system failure, necessitating its study in order to prevent future failures. Two rigid disks mounted to both ends of a double-overhung flexible shaft system are investigated for coupled torsional-transverse vibration. The equations of motion were created by applying the kinematic restrictions and the Hamilton equation to the energy expressions. The governing equation is divided into various orders when the displacement is expressed as a perturbation series. This demonstrated second and higher-order torsional and transverse term interactions. In order to comprehend the connection better, rigid.

Keywords
Double Overhung, Coupled, Vibration, Campbell

1. Introduction

An area of study within the boarder subject of mechanical engineering is transverse vibration modal analysis of centrifugal blowers with overhung shaft bearing rotor orientation. In commercial and industrial contexts, centrifugal blowers are machinery used to move air or other gases. These devices typically consist of a rotor that is operated by an electric motor and spins rapidly. The arrangement of the shaft and bearings used to support the rotor in the blower is referred to as the "overhung shaft bearing rotor orientation."

The transverse vibration of the modal analysis of Double overhung centrifugal blower mainly focuses on the development of mathematical models to predict the mode of vibration and their respective natural frequencies and experimental investigation of the transverse vibration behaviour of overhung centrifugal blowers. A study by (Hao) used the Transfer Matrix Method to establish a numerical model of air blower systems and found out mode shape, critical speed and unbalanced reaction[1]. S L Ajit Prasad investigated a spinning mechanical system with an imbalanced rotor installed on an overhanging shaft to determine its vibrational properties[2]. More studies about the influence of impeller blade thickness and rotating speed on the performance of the impeller through an experimental and numerical analysis[3]. Sailendra Shah used Transfer Matrix to perform modal analysis of the offset rotor shaft of a large centrifugal fan and compared the result with Numerical simulation from ANSYS Workbench[4].

This research work focuses on the development of an equation of motion using the Hamilton Principle for double overhung centrifugal blower and a perturbation series would be employed to decouple the first-order and second-order equation and identify the interaction of transverse vibration on torsional vibration and vice versa.

2. Methodology

The following research methodology is adopted for this paper. From libraries and the internet, we collected the prior research studies and other pertinent publications. We used the previous thesis from the Institute of Engineering and their access to many foreign magazines. The FD fan utilized for the

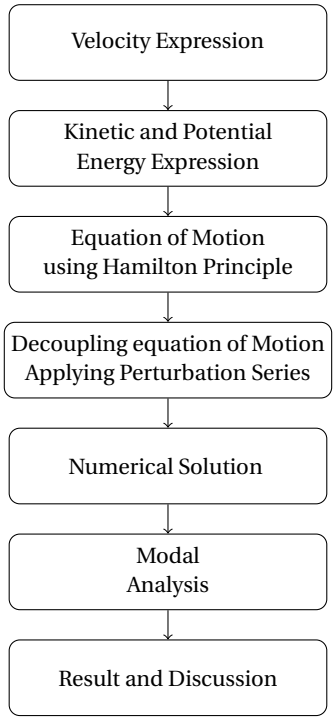

Figure 1: Methodology

cyclone separator in the Eastern Cosmos Cements was used to collect data on measurement and material properties. A mathematical model was created, and perturbation series were employed to decouple the equations for the study of the interaction of transverse vibration on torsional vibration and vice versa. A simulated modal analysis of the FD fan with the same geometry and material was performed using ANSYS Workbench. The twin overhung rotor shaft FD fan modal analysis also made use of ANSYS. The results of the numerical analysis and the simulation work were compared and verified and operational ranges of the speed of the fan were thus obtained.

3. Mathematical Modeling

3.1 Coordinate system

Let the fixed coordinate system OXYZ be an inertial frame of reference. An element of the shaft is considered to be a disk of infinitesimal thickness and is located with the help of displacement and rotation[5].

$$\mathrm{R}_{321}(\emptyset,\theta,\Psi) = \mathrm{R}_1(\emptyset)\mathrm{R}_2(\theta)\mathrm{R}_3(\psi) \tag{1}$$

$$R_1(\emptyset) = \begin{bmatrix} 1 & 0 & 0 \\ 0 & \cos\emptyset & \sin\emptyset \\ 0 & -\sin\emptyset & \cos\emptyset \end{bmatrix} \tag{2}$$

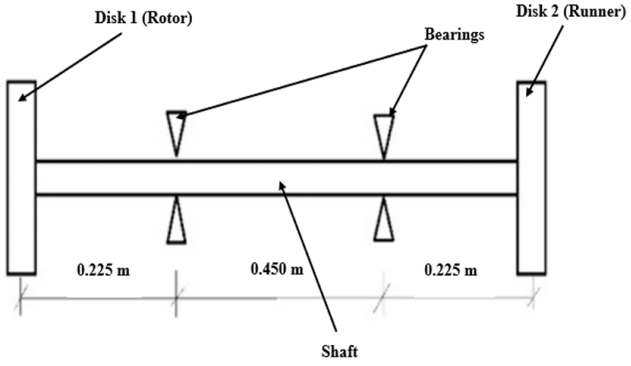

Figure 2: Double overhung System

$$R_2(\theta) = \begin{bmatrix} \cos\theta & 0 & -\sin\theta \\ 0 & 1 & 0 \\ \sin\theta & 0 & \cos\theta \end{bmatrix} \tag{3}$$

$$R_3(\psi) = \begin{bmatrix} \cos\psi & \sin\psi & 0 \\ -\sin\psi & \cos\psi & 0 \\ 0 & 0 & 1 \end{bmatrix} \tag{4}$$

$$\mathrm{R}_{321} = \begin{bmatrix} C\theta C\psi & C\theta S\psi & -S\theta \\ -C\phi S\psi + C\psi S\theta S\phi & C\psi C\phi + S\psi S\theta S\phi & S\psi C\theta \\ S\phi S\psi + C\phi S\theta C\psi & -S\phi C\psi + C\phi S\theta S\psi & C\phi C\theta \end{bmatrix} \tag{5}$$

Here cosine and sine are represented by C and S respectively.

3.2 Velocity Expression

The vector sum of time gives the expression for the angular velocity of the system [6].

$$\omega = \dot{\boldsymbol{\psi}} + \dot{\boldsymbol{\theta}} + \dot{\emptyset} \tag{6}$$

x, y and z components of angular velocity can be identified as [7]:

$$\begin{bmatrix} \omega_x \\ \omega_y \\ \omega_z \end{bmatrix} = \begin{bmatrix} \dot{\phi} - \dot{\psi}\sin\theta \\ \dot{\theta}\cos\phi + \dot{\psi}\cos\theta \\ -\dot{\theta}\sin\phi + \dot{\psi}\cos\theta\sin\phi \end{bmatrix} \tag{7}$$

x, y and z components of Linear velocity when velocity along x-axis is ($\dot{}$u) = 0 is as [8].

$$\begin{bmatrix} V_x \\ V_y \\ V_z \end{bmatrix} = \begin{bmatrix} v\dot{\psi} - (w\theta)\dot{\phi} \\ v\dot{\phi}\cos\theta + w\dot{\psi}\sin\theta \\ -v\dot{\phi}\sin\theta + w\dot{\psi}\cos\theta \end{bmatrix} \tag{8}$$

3.3 Kinematic Constraints

A shaft longitudinal axes are aligned with the x-axis and vibration is experienced along the perpendicular axes y and z.u,v and w are displacement along x,y and z axes respectively where displacement along x-axes is taken as zero. θ, ϕ and ψ is the rotation along the x,y and z axes respectively. The relation between θ, ψ and their first and second derivative with respective displacement is given by [9]:

$$\theta = \frac{\partial w}{\partial x}; \quad \dot{\theta} = \frac{\partial \dot{w}}{\partial x} = (\dot{w})'; \quad \ddot{\theta} = \frac{\partial \ddot{w}}{\partial x} = (\ddot{w})'.$$

$$\psi = -\frac{\partial v}{\partial x}; \quad \dot{\psi} = -\frac{\partial \dot{v}}{\partial x} = (\dot{v})'; \quad \ddot{\psi} = -\frac{\partial \ddot{v}}{\partial x} = -(\ddot{v})'. \tag{9}$$

3.4 Kinetic and potential energy

3.4.1 Kinetic energy of shaft

The kinetic energy of the shaft for torsional and lateral vibrations is given as [10].

$$\mathrm{T} = \frac{1}{2}\rho A\int_0^{\mathrm{L}} \mathrm{V}^2\mathrm{dx} + \frac{1}{2}\mathrm{I_p}\int_0^{\mathrm{L}} \mathrm{w_x^2 dx} + \frac{1}{2}\mathrm{I_d}\int_0^{\mathrm{L}} \left(\mathrm{w_y^2} + \mathrm{w_z^2}\right)\mathrm{dx} \tag{10}$$

$$\mathrm{T} = \frac{1}{2}\rho A\int_0^{\mathrm{L}} \left[\dot{\mathrm{w}}^2 + \dot{\mathrm{v}}^2 + \dot{\mathrm{v}}^2\theta^2\psi^2 + \dot{\mathrm{v}}^2\psi^2 + \dot{\mathrm{w}}^2\theta^2\right]\mathrm{dx} + \frac{1}{2}\mathrm{I_p}\int_0^{\mathrm{L}} \left[\Omega^2 - 2\Omega\theta\dot{\psi}\right]\mathrm{dx} + \frac{1}{2}\mathrm{I_d}\int_0^{\mathrm{L}} \left[\theta^2 + \psi^2\right]\mathrm{dx} \tag{11}$$

where, $V^2 = \dot{w}^2 + \dot{v}^2 + \dot{v}^2\theta^2\Psi^2 + \dot{v}^2\Psi^2 + \dot{w}^2\theta^2$

3.4.2 Potential Energy of shaft

The potential energy of the shaft for transverse deflection and the torsional condition is as follows [11].

$$\mathrm{U} = \frac{\mathrm{EI}}{2}\int_0^{\mathrm{L}} \left[\left(\frac{\partial^2 \mathrm{u}}{\partial \mathrm{x}^2}\right)^2 + \left(\frac{\partial^2 \mathrm{v}}{\partial \mathrm{x}^2}\right)^2\right]\mathrm{dx} + \frac{\mathrm{GJ}}{2}\int_0^{\mathrm{L}} \left(\frac{\partial \phi}{\partial \mathrm{x}}\right)^2 \mathrm{dx} \tag{12}$$

3.4.3 KE of disk 1

Kinetic energy for the disk at the location at X=0 is given as follows [11].

$$T_{d1} = \frac{1}{2}M_{d1}\left(\dot{v}^2 + \dot{w}^2\right)\Big|_{x=0} + \frac{1}{2}I_{pd1}\omega_x^2\Big|_{x=0} + \frac{1}{2}I_{dd1}\left(\omega_y{}^2 + \omega_z{}^2\right)\Big|_{x=0} \quad (13)$$

3.4.4 KE of disk 2

Kinetic energy of a diak at location x=L is given as follows [11].

$$T_{d2} = \frac{1}{2}M_{d2}\left(\dot{v}^2 + \dot{w}^2\right)\Big|_{x=L} + \frac{1}{2}I_{pd2}\omega_x^2\Big|_{x=L} + \frac{1}{2}I_{dd2}\left(\omega_y{}^2 + \omega_z{}^2\right)\Big|_{x=L} \quad (14)$$

3.5 Equation of Motion and Perturbation series

Applying Hamilton's principle to energy expression results to Equation of motion and boundary conditions for the system. For a clear understanding of the nature of the equation of motion derived, we need to apply perturbation. Perturbation helps to decouple the equation into first-order, second-order and higher order equations.

$$v = \varepsilon v_1 + \varepsilon^2 v_2 + \cdots + \varepsilon^n v_n + \cdots \quad (15)$$

$$w = \varepsilon w_1 + \varepsilon^2 w_2 + \cdots + \varepsilon^n w_n + \cdots \quad (16)$$

$$\theta = \varepsilon\theta_1 + \varepsilon^2\theta_2 + \cdots + \varepsilon^n\theta_n + \cdots \quad (17)$$

3.5.1 First order equation

After substituting values from equations (15),(16) and (17) in the equation of motion, we can get the following three equations.

$$\begin{aligned}&(EIv_1'')'' + \rho A\ddot{v}_1 - (I_d\ddot{v}_1')' - (I_p\Omega\dot{w}_1')' = -M_{d1}\ddot{v}_1\delta(x-0)\\ &- M_{d2}\ddot{v}_1\delta(x-L) + (I_{dd1}\ddot{v}_1')'\delta(x-0) + (I_{dd2}\ddot{v}_1')'\delta(x-L)\\ &+ (I_{pd1}\Omega\dot{w}_1')'\delta(x-0) + (I_{pd2}\Omega\dot{w}_1')'\delta(x-L)\end{aligned} \quad (18)$$

$$\begin{aligned}&(EIw_1'')'' + \rho A\ddot{w}_1 - (I_d\ddot{w}_1')' + (I_p\Omega\dot{v}_1')' =\\ &- Md_1\ddot{w}_1\delta(x-0) - Md_2\ddot{w}_1\delta(x-0) + (I_{dd1}\ddot{w}_1')'\\ &\delta(x-0) + (I_{dd2}\ddot{w}_1')'\delta(x-L) - (I_{pd1}\Omega\dot{v}_1')'\delta(x-0)\\ &- (I_{pd2}\Omega\dot{v}_1')'\delta(x-L)\end{aligned} \quad (19)$$

$$(GJ\phi_1')' - I_p\ddot{\phi}_1 = I_p d_1\ddot{\phi}_1\delta(x-0) + I_p d_2\ddot{\phi}_1\delta(x-L) \quad (20)$$

There is no torsional term in transverse vibration equation and vice versa.this shows that there is no interaction between transverse and torsional vibration.

3.5.2 Second order Equation

The first-order equation after decoupling is given as follows.

$$\begin{aligned}&(EIv_2'')'' + \rho A\ddot{v}_2 - (I_d\ddot{v}_2')' - (I_p\Omega\dot{w}_2')' = (I_p\ddot{\phi}_1 w_1')'\\ &+ (I_p\dot{\phi}_1\dot{w}_1')' - M_{d1}\ddot{v}_2\delta(x-0) - M_{d2}\ddot{v}_2\delta(x-L)\\ &+ \left(I_{dd1}\ddot{v}_2'\right)'\delta(x-0) + (I_{dd2}\ddot{v}_2')'\delta(x-L) + (I_{pd1}\ddot{\phi}_1 w_1')'\\ &\delta(x-0) + (I_{pd2}\ddot{\phi}_1 w_1')'\delta(x-L) + (I_{pd1}\Omega\dot{w}_2')'\delta(x-0)\\ &+ (I_{pd2}\Omega\dot{w}_2')'\delta(x-L) + +(I_{pd1}\dot{\phi}_1\dot{w}_1')'\delta(x-0)\\ &+ (I_{pd2}\dot{\phi}_1\dot{w}_1')'\delta(x-L)\end{aligned} \quad (21)$$

$$\begin{aligned}&(EIv_2'')'' + \rho A\ddot{w}_2 - (I_d\ddot{w}_2')' + (I_p\Omega\dot{v}_2')' + (I_p\dot{\phi}_1\dot{v}_1')'\\ &= -M_{d1}\ddot{w}_2\delta(x-0) - M_{d2}\ddot{w}_2\delta(x-L) + (I_{dd1}\ddot{w}_2')'\\ &\delta(x-0) + (I_{dd2}\ddot{w}_2')'\delta(x-L) - (I_{pd1}\Omega\dot{v}_2')'\delta(x-0)\\ &- (I_{pd2}\Omega\dot{v}_2')'\delta(x-L) - (I_{pd1}\dot{\phi}_1\dot{v}_1')'\delta(x-0)\\ &- (I_{pd2}\dot{\phi}_1\dot{v}_1')'\delta(x-L)\end{aligned} \quad (22)$$

$$\begin{aligned}&(GJ\phi_2')' - I_p\ddot{\phi}_2 =\\ &I_p\frac{\partial}{\partial t}(\dot{v}_1{}'w_1') + I_{pd1}\ddot{\phi}_2\delta(x-0) + I_{pd2}\ddot{\phi}_2\delta(x-L) +\\ &I_{pd1}\frac{\partial}{\partial t}(\dot{v}_1{}'w_1')\delta(x-0) + I_{pd2}\frac{\partial}{\partial t}(\dot{v}_1{}'w_1')\delta(x-L)\end{aligned} \quad (23)$$

Equation (21), (22) and (23) shows that there is torsional term in the first two transverse equation and there is transverse term in the third torsional vibration equation. This shows that we can easily decouple equations of transverse vibration and torsional vibration separately. The nature of the equation shows that there is interaction of transverse vibration in torsional vibration and vice versa.

4. Analytical Solution

for the solution of the first-order equation, the polynomial function for the mode shape is identified using the assumed mode method. The polynomial function after applying boundary condition for the double overhung condition is given by [12].

$$\emptyset = x^6 - 3Lx^5 + \frac{5L^2}{2}x^4 - \frac{L^5}{2}x + \frac{483L^6}{4096}$$

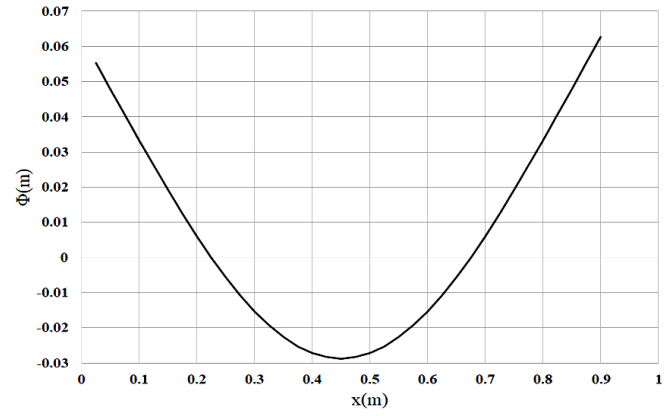

Figure 3: Mode shape analytically

The mode shape of the double overhung system shows that displacement is maximum at the middle and end of the shaft. Displacement at the end of the shaft depends upon the mass of both disks.

4.1 Equivalent System parameter

Applying the orthogonality condition, equation of motion for transverse vibration can reduce to a couple system of ODE from couple system of PDE as [13]:

$$M_n\ddot{V}_n(t) + C_n\dot{W}_n(t) + K_nV(t) = 0$$

$$M_n\ddot{W}_n(t) - C_n\dot{V}_n(t) + K_nV(t) = 0$$

4.1.1 Mass

$$M_{\text{eq}} = -(\rho A + M_{\text{d1}} + M_{\text{d2}}\frac{448819193}{151145938944}L^{13} + (I_d + I_{dd1} + I_{dd2})\frac{10}{7}L^9 \quad (24)$$

4.1.2 Damping Constant

$$C_{\text{eq}} = -\Omega\left(I_p + I_{\text{pd1}} + I_{\text{pd2}}\right)\frac{10}{7}L^9 \quad (25)$$

4.1.3 Stiffness

$$K_{\text{eq}} = 720 \cdot EI \cdot L^5 \quad (26)$$

4.1.4 Model Parameter

The parameters shown in Table 1 are considered for the solution which was collected from the Eastern Cosmos Cement PVT LTD, Morang.

Table 1: Model Parameters

Parameters	Values
Diameter of shaft (ds)	0.075 m
Density of shaft material(ρ)	7860 kg/m^3
Cross section of shaft(A)	0.0044 M2
Length of shaft(L)	0.9 m
Mass per unit length of shaft (m)	34.71 kg/m
Total mass of shaft(M)	31.24 kg
Shear modulus of shaft(G)	84 GPA
Modulus of Elasticity of shaft (E)	202 GPA
AMOI of shaft section(Id)	1.55×10^{-6} M4
polar AMOI of the shaft section (Ip)	3.11×10^{-6} M4
mass of Disk 1 (md1)	55.55 Kg
mass of Disk 2 (md2)	443.91 Kg
Diametrical MMOI of Disk 1 (Idd1)	0.358 kg m^2
Diametrical MMOI of Disk 2 (Idd2)	0.624 kg m^2
Polar MMOI of disk 1 (Ipd1)	40.07 kg m^2
Polar MMOI of disk 2 (Ipd2)	79.9 kg m^2
Rotating speed	2080 RPM
Rate of Flow	(22702-42093) m^3/h
Full Pressure	4181/3066 pa
Power	55 Kw

4.1.5 Mass

Applying parameter values in equation (24) gives equivalent value of mass for given system.

$$M_{1\text{eq}} = -8579.18$$

4.1.6 Damping Constant

Applying parameter values in equation (25) gives equivalent value of damping constant in term of rotational speed Ω.

$$C_{1\text{eq}} = 13649.29\Omega$$

4.1.7 Stiffness

Applying parameter values in equation (26) gives equivalent value of stiffness of the system.

$$K_{1\text{eq}} = 3205702386$$

5. Simulation

Simulation work was done in ANSYS 2019R3 Workbench for the validation of the mathematical model. The geometry was prepared from the parameter of the force draft fan collected from the Eastern Cosmos Cement. Followed by ANSYS workbench automated Meshing. Remote displacement was set to zero for all axis in both bearings. Velocity vector was given to the whole system along the X-axis. Transverse vibration along y-axis and z-axis were considered but vibration along x-axis was set to zero for the system.

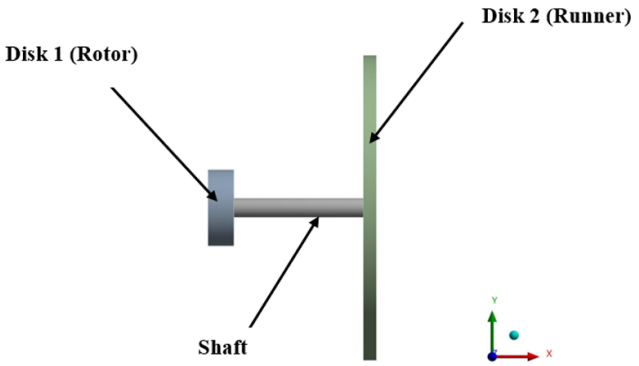

Figure 4: Geometry

6. Result and Discussion

The operating speed of the centrifugal fan is 2080 RPM(218 rad/sec). The critical frequency obtained from the analytical solution is 3621 RPM (379 rad/sec) which is close to the 3532 RPM(369.76 rad/sec) value obtained from ANSYS. Error is in the acceptable range of 2.45 per cent. This result shows that the operating speed is in the range of the safe zone.

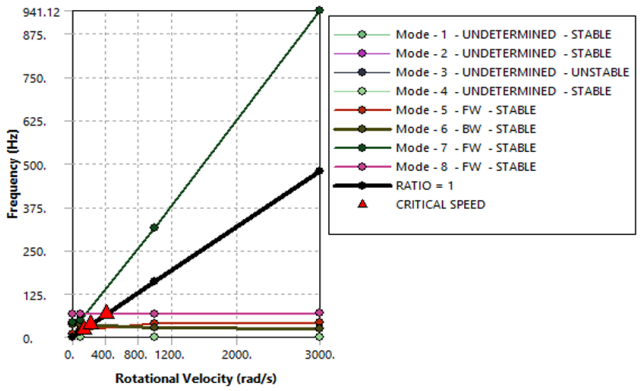

Figure 5: ANSYS Campbell Diagram

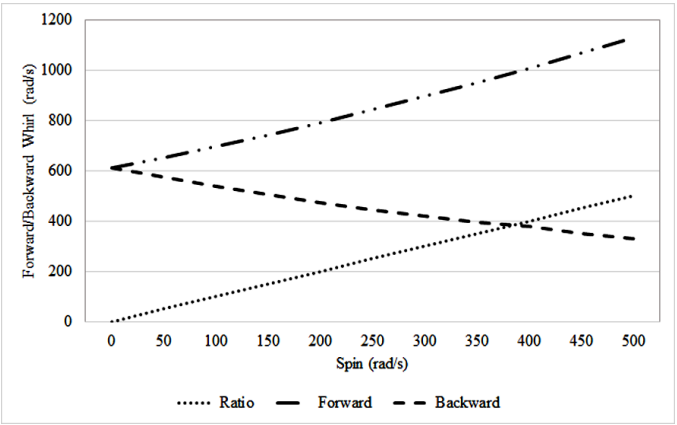

Figure 6: Forward and Backward Whirl with Spin

7. Conclusion

The torsional flexure interaction of the shaft-disk system was studied by modeling the shaft as a rotating Euler-Bernoulli beam and the disk as rigid. The governing equations of the system for coupled vibrations are found to be a coupled system of partial differential equations. It is clearly shown that the interaction of torsional and transverse vibration doesn't occur in first order and it is clearly seen in second order equation. For a spin speed of 2080 RPM(218 rad/sec), the Natural Frequency for first-order free transverse vibration is found to be 27929 rad/s and 30203 rad/s. The critical frequency for backward whirl is found to be 3621 RPM(379rad/s) and the forward frequency is above 379 rad/sec.

References

[1] Hao Wu, Qiong Zhou, Zhiming Zhang, and Qi An. Vibration analysis on the rolling element bearing-rotor system of an air blower. *Journal of mechanical science and technology*, 26:653–659, 2012.

[2] N Ahobal et al. Study of vibration characteristics of unbalanced overhanging rotor. In *IOP Conference Series: Materials Science and Engineering*, volume 577, page 012140. IOP Publishing, 2019.

[3] Kiran C More, Sachin Dongre, and Gaurav P Deshmukh. Experimental and numerical analysis of vibrations in impeller of centrifugal blower. *SN Applied Sciences*, 2(1):82, 2020.

[4] Shailendra Shah and Mahesh Chandra Luintel. Transverse vibration modal analysis on offset rotor shaft of large centrifugal fan. In *Proceedings of IOE Graduate Conference*, 2019.

[5] H Alemi Ardakani and TJ Bridges. Review of the 3-2-1 euler angles: a yaw-pitch-roll sequence. *Department of Mathematics, University of Surrey, Guildford GU2 7XH UK, Tech. Rep*, 2010.

[6] T Greenwood Donald. *Principles of Dynamics*. Prentice-Hall, 2003.

[7] PVDL Paulo. A time-domain methodology for rotor dynamics: analysis and force identification. *Univeridade Tecnica de Lisboa, Portugal*, 2011.

[8] Sushant Poudel and Mahesh Chandra Luintel. Coupled lateral and torsional vibration of a rigid disk attached to a flexible shaft. 2022.

[9] Raman Koirala and Mahesh Chandra Luitel. Dynamic response of vertical shaft pelton turbine unit for forced vibration. *Journal of Innovations in Engineering Education*, 4(1):34–41, 2021.

[10] Janak Kumar Tharu, Nishant Bhatta, Sanjeev Karki, and Mahesh Chandra Luintel. Free vibration analysis of simply supported pelton turbine: A case of flexible rotor bearings. In *Proceedings of IOE Graduate Conference*, 2019.

[11] Reewaj Bhandari, Mahesh Chandra Luintel, and Kamal Pokhrael. Dynamic response of overhung pelton turbine unit for forced vibration. In *Proceedings of IOE Graduate Conference*, volume 6, pages 69–75, 2019.

[12] Mahesh Chandra Luintel. Development of polynomial mode shape functions for continuous shafts with different end conditions. *Journal of the Institute of Engineering*, 16(1):151–161, 2021.

[13] Bidhan Pandey. *Vibration analysis of cantilever shaft-disk system for transient response to impact jet*. PhD thesis, IOE Pulchowk Campus, 2023.